

Development of supramolecular structure through alkylation of pendant pyridyl functionality

Edwin C. Constable,^{*a,b} Catherine E. Housecroft,^{a,b} Markus Neuburger,^b David Phillips,^c Paul R. Raithby,^c Emma Schofield,^b Emma Sparr,^c Derek A. Tocher,^d Margareta Zehnder^b and Yves Zimmermann^b

^a School of Chemistry, University of Birmingham, Edgbaston, Birmingham, UK B15 2TT.
E-mail: e.c.constable@bham.ac.uk

^b Institut für Anorganische Chemie, Spitalstrasse 51, CH 4056 Basel, Switzerland

^c University Chemical Laboratory, Lensfield Road, Cambridge, UK CB2 1EW

^d Department of Chemistry, University College London, 20 Gordon Street, London, UK WC1H 0AJ

Received 3rd February 2000, Accepted 14th April 2000

Published on the Web 8th June 2000

The complex $\mathbf{1}^{2+}$ which has two pendant 4-pyridyl substituents may be viewed as a metal-containing analogue of 4,4'-bipyridine. The complex undergoes *N*-alkylation reactions with a variety of alkylating agents to give more highly functionalised tetracationic complexes which may be termed *metalloviologens* by analogy with viologens. These complexes may also be prepared by alkylation of the free ligands and subsequent coordination of the pendant quaternised ligand. Structural studies have established that the *N*-alkylated complexes possess the correct spatial characteristics for the preparation of metallocycles analogous to known cyclic bis(4,4'-bipyridinium) species which possess useful molecular recognition properties.

The metal-directed assembly of supramolecular structures is a well-established synthetic methodology and has been used *inter alia* for the preparation of helices,^{1,2} catenanes³ and rotaxanes,⁴ boxes and polygons,^{5,6} cylinders,⁷ dendrimers⁸ and extended two- or three-dimensional lattices.⁷ The assembly paradigms are based upon the coordination requirements and properties of the metal centres and the donor properties of the ligands. These are reasonably well understood and the study of their interplay may be referred to as *metallo-supramolecular chemistry*.⁹ One of the limiting features of the metal-directed approach is the need to prepare functional and often highly reactive ligand species; on many occasions, the functionality within the supramolecule is incompatible with the conditions required for coordination to the desired metal centre. At the same time as developing the now-conventional metallocyclic approaches, we have been exploring assembly methodologies based upon reactions of coordinated ligands^{10–12} and in this paper we describe a series of *N*-alkylation reactions of the pendant 4-pyridyl groups in the complex cation $[\text{Fe}(\mathbf{I})_2]^{2+}$ $\mathbf{1}^{2+}$ (\mathbf{I} = 4'-(4-pyridyl)-2,2':6',2''-terpyridine) and show that these facile reactions allow the introduction of functional substituents. We also show that 4,4'-bipyridinium and *N*-alkylated derivatives of $\mathbf{1}^{2+}$ are equivalent motifs allowing the prospect of preparing metallocyclic polygons related to the macrocyclic 4,4'-bipyridinium systems reported by Stoddart and Philp.¹³

Results and discussion

Strategy

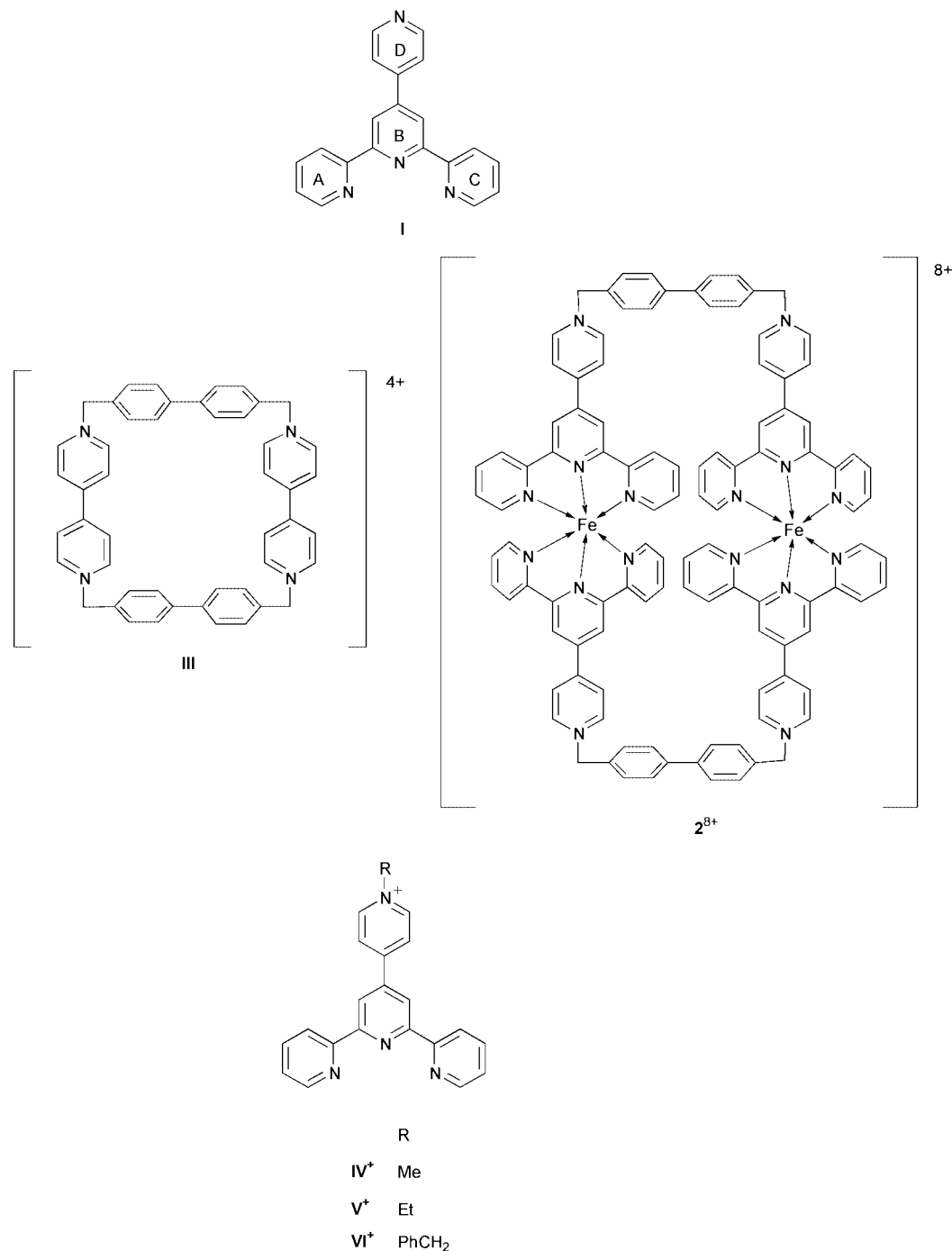
The ligand \mathbf{I} with a pendant 4-pyridyl group is readily prepared by Kröhnke methodology from 2-acetylpyridine and pyridine-4-carboxaldehyde^{11,14} and gives diamagnetic low spin 2:1 iron(II) complexes $[\text{Fe}(\mathbf{I})_2]^{2+}$ $\mathbf{1}^{2+}$ upon reaction with iron(II) salts.¹¹ We reasoned that the linear arrangement of the two 4-pyridyl groups in $\mathbf{1}^{2+}$ cations made this complex a metal-containing topographical analogue of 4,4'-bipyridine \mathbf{II} (Fig. 1). *N,N'*-Dialkyl-4,4'-bipyridinium salts (viologens) are

widely used as electron-transfer agents in photocatalytic systems¹⁵ and as structural motifs in supramolecular systems.¹³ We were particularly interested in using *N,N'*-dialkylated units derived from \mathbf{I} instead of 4,4'-bipyridinium motifs in the preparation of metal-containing supramolecular systems and chose the molecular box \mathbf{III} ¹³ as our target with the aim of preparing the analogous $\mathbf{2}^{8+}$.¹⁶ In this paper, we probe the methods for the preparation of, and discuss the properties of, mononuclear metalloviologens.

Preliminary studies involving the methylation of the pendant 4-pyridyl groups in $\mathbf{1}^{2+}$ had established that quaternisation reactions lead to metal-containing analogues of methyl viologen (*N,N'*-dimethyl-4,4'-bipyridinium salts)¹¹ and had shown that the replacement of the C–C bond in \mathbf{II} by the dicationic $\{\text{Fe}(\text{terpy})_2\}$ moiety did not significantly reduce the nucleophilicity of the pendant group. Electrochemical and spectroscopic studies indicated a significant degree of interaction between the terpy metal-binding domain and the pendant pyridine or *N*-methylated pyridine rings but we were unable to obtain X-ray quality crystals to unambiguously establish the solid state structure. In the course of related studies exploring the analogy between $\mathbf{1}^{2+}$ and \mathbf{II} , we obtained good quality crystals of $\mathbf{I}[\text{NO}_3]_2$ from the reaction of $\mathbf{I}[\text{PF}_6]_2$ with cadmium nitrate and the solid state structure of this salt is discussed later.

Conformation of \mathbf{I}

One of the questions relating to the viologen–metalloviologen analogy is the degree of electronic interaction between (a) the pendant 4-pyridyl/4-pyridinium rings and the terpy metal-binding domain and (b) the interaction between the two \mathbf{I} ligands when they are coordinated to a single metal centre. In preliminary studies we have determined the solid state structure of ligand \mathbf{I} . The solid state structure of \mathbf{I} is shown in Fig. 2. The terpy domain adopts the expected *trans,trans* conformation¹⁷ and is approximately planar with an angle of 10.69° between the least squares planes of the A (C) rings and the B ring. The 4-pyridyl substituent is twisted with respect to the terpy domain



(least squares planes: B ring–D ring, 26.37°; D ring—all terpy non-H atoms, 24.85°). There are no unusual intermolecular contacts within the lattice.

N-Alkylation of I

In principle, ligand **I** has three possible sites of *N*-alkylation—rings A/C, B or D. When we commenced this work, we did not consider that regioselective alkylation of **I** would be successful and anticipated mixtures of A/C and D-ring alkylated compounds on steric grounds. After the bulk of the experimental work described in this paper was completed, we performed a series of calculations to determine the degree of electronic interactions between the substituents in our new complexes, and in the course of these studies we noted that the free ligand **I** had a significant localisation of electron density on the D-ring nitrogen atom and considered that regioselective alkylation might be possible.

The reaction of **I** with MeI in acetonitrile proceeded smoothly to give a yellow solution, from which salt **IV**[PF₆]₄ was isolated in 44% yield as a golden yellow solid. The ¹H NMR spectrum indicated that a highly symmetrical product had been obtained, consistent with monoalkylation on ring B or D. The shift differences unambiguously establish alkylation on the pendant D-ring. The compound was fully characterised and data are presented in the Experimental section. This complex is an analogue of methyl viologen, in which only one of the pyridine rings is alkylated. As such the compound is expected to be electrochemically active, and cyclic voltammetry revealed essentially reversible processes at –1.33 and –1.95 V (Table 1, MeCN, potentials quoted *versus* Fc⁺/Fc). These electrochemical data may usefully be compared with some model compounds to assess whether the *N*-alkylated ligand shows viologen-like properties. Methyl viologen (*N,N'*-dimethyl-4,4'-bipyridinium) salts exhibit reversible reduction processes at –0.98 and –1.34 V (H₂O, potentials adjusted from NHE using

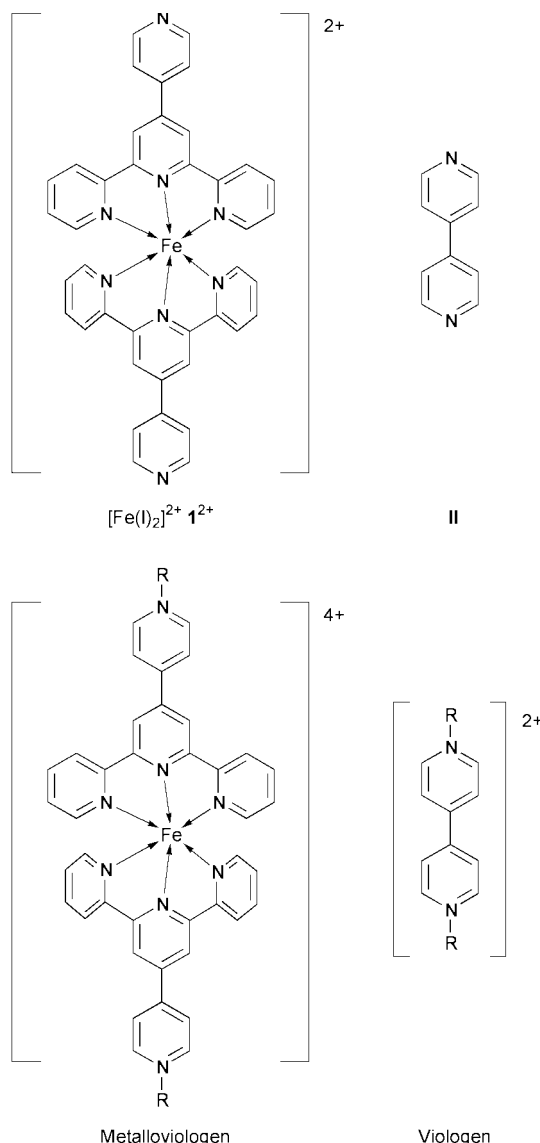


Fig. 1 The analogy between the iron complex I^{2+} and 4,4'-bipyridine (**II**) extends to the *N*-alkylated species and leads to the description of the complexes as metalloviologens.

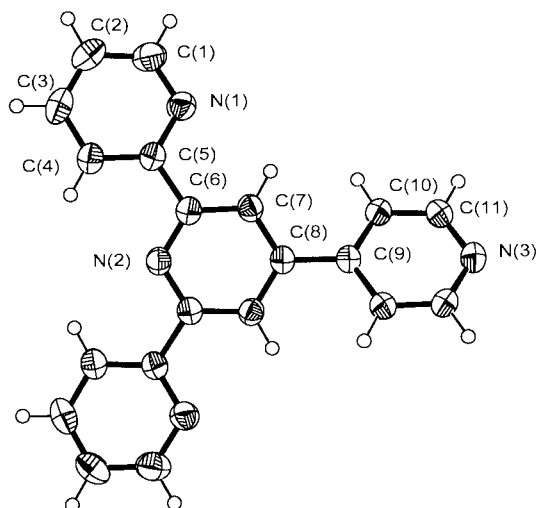


Fig. 2 Molecular structure of **I** showing the numbering scheme adopted. Thermal ellipsoids at 50% probability.

the value of +0.548 for the Fc^+/Fc couple in MeCN and ignoring any liquid junction potentials).¹⁵ In contrast, MeCN solutions of *N*-methylpyridinium salts exhibit a reduction at

Table 1 Electrochemical data^a

	<i>E</i> /V
IV [PF ₆]	−1.33, −1.95
VI [PF ₆]	−1.27, ^b −1.97, −2.13 ^b
[Fe(terpy) ₂][PF ₆] ₂	+0.74, −1.64, −1.82
1 [PF ₆] ₂	+0.80, −1.51, −1.66
2 [PF ₆] ₄	+0.84, −1.08, −1.54
3 [PF ₆] ₄	+0.89, −1.05, −1.50
4 [PF ₆] ₄	+0.88, −1.03, absorption (−1.60 forward, −1.39 return)
5 [PF ₆] ₄	+0.88, −1.06, −1.49
6 [PF ₆] ₄	+0.89, −1.04, −1.49, −1.81
7 [PF ₆] ₄	+0.84, −1.06, −1.52 (−1.11, ^b −1.26, ^b −1.72 ^b)
8 [PF ₆] ₄	+0.84, −1.07, −1.54
9 [PF ₆] ₄	+0.82, −1.04, −1.48

^a Unless otherwise stated, platinum bead electrodes were used, MeCN solvent, potentials quoted are *versus* Fc^+/Fc . ^b Glassy carbon working electrode.

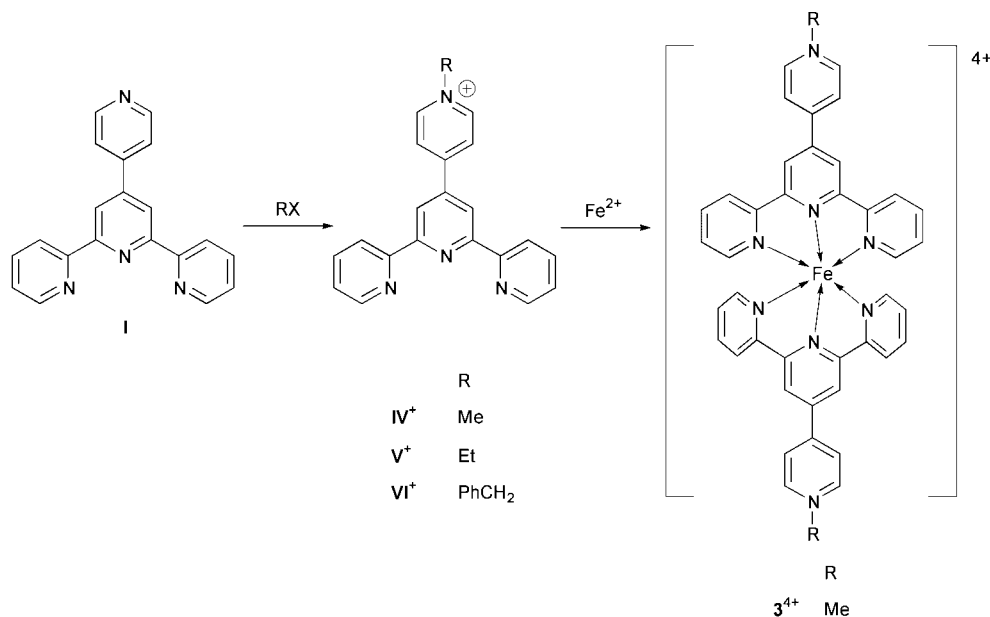
−1.52 V (*versus* Fc^+/Fc).¹⁸ The *N*-alkylated ligand is closer in behaviour to the monoalkylated model compound, although the extended conjugation associated with the aromatic substituents in the 2- and 6-positions stabilises the radical. These results suggest that viologens (and by analogy, metalloviologens) based on **I** will be more readily reduced than simple 4,4'-bipyridinium systems.

The analogous salts **V**[PF₆] and **VI**[PF₆], both alkylated on the D ring, were prepared by reaction with iodoethane or benzyl bromide respectively, followed by precipitation of the hexafluorophosphate salts (Scheme 1). Characterisation data for the compounds are presented in the Experimental section. The cyclic voltammogram of **VI**[PF₆] revealed reversible processes at −1.27, −1.97 and −2.13 V. The benzyl salt **VI**[PF₆] was of particular interest as it contained the motif which we planned to incorporate into the metallomacrocyclic. Detailed discussion of the spectroscopic properties of this model compound will be presented later. We also considered that the compound could provide valuable geometrical information which would help our ligand design and we accordingly determined the structure of the salt **VI**[PF₆].

The structure of the **VI**⁺ cation in the salt **VI**[PF₆] is presented in Fig. 3. All bond lengths and angles are within the usual bounds. Any interest lies in the spatial arrangement of the aromatic rings in the cation and in the packing of the cations within the crystal lattice. The terminal rings of the terpy ligand are crystallographically independent and the least squares planes between the A and C rings and the B ring are 1.57° and 15.00°. The least squares planes angle between the B and D rings is 36.2°, at the conventional limit for conjugation. The methylene group of the benzyl substituent introduces a significant twisting, quantified in the torsion angle C(19)–N(4)–C(21)–C(22) of 52.8°; the result is that the A and E rings are almost perpendicular. There are a number of interionic interactions within the solid state. Adjacent pairs of cations show a stacking interaction between coplanar phenyl rings of the benzyl substituents (interplanar separation of 3.59 Å, Fig. 4a). A second stacking interaction occurs between bipy moieties of other adjacent pairs, with A···B' and B···A' (Fig. 4b). The cation adopts an L-shaped structure, in which the short bar of the L is the phenyl group, perpendicular to the terpy. In combination with the other intercation interactions, this creates a cavity into which the terminal pyridine of the next cation fits snugly (Fig. 4c) with the shortest contact being 2.37 Å between H^{5A} of the guest ring and H^{3B} of the host.

N-Alkylation of **1**[PF₆]₂

The *N*-methylation of **1**[PF₆]₂ proceeds smoothly upon reaction with MeI in acetonitrile to give a blue solution containing **3**⁴⁺,¹¹



Scheme 1

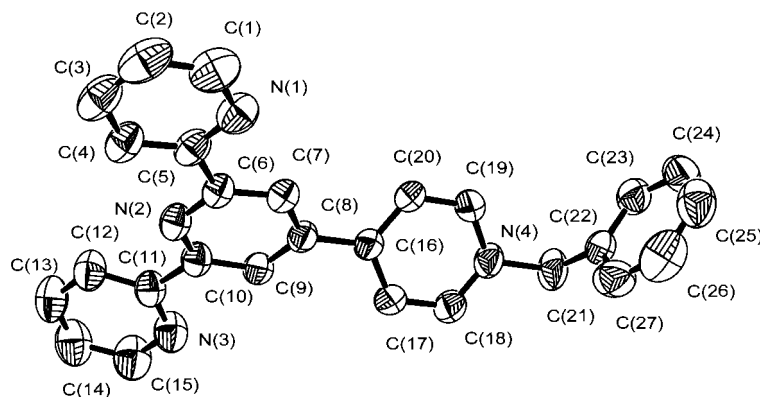


Fig. 3 Molecular structure of the VI⁺ cation in the salt VI[PF₆] showing the numbering scheme adopted. Hydrogen atoms have been omitted for clarity; thermal ellipsoids at 50% probability.

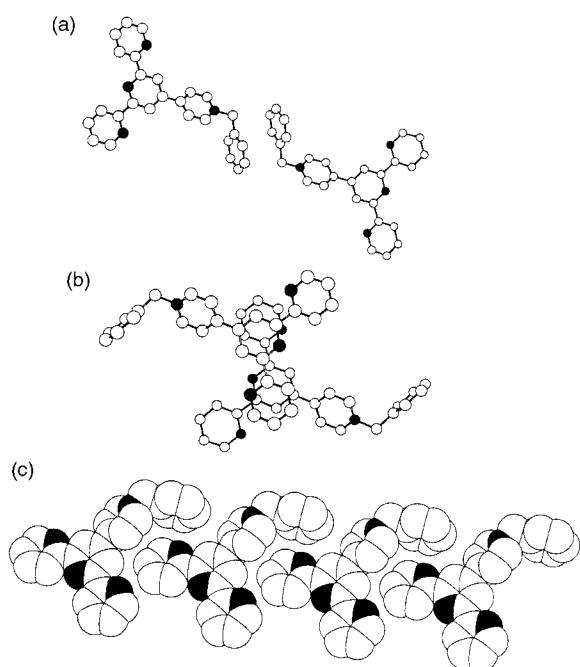
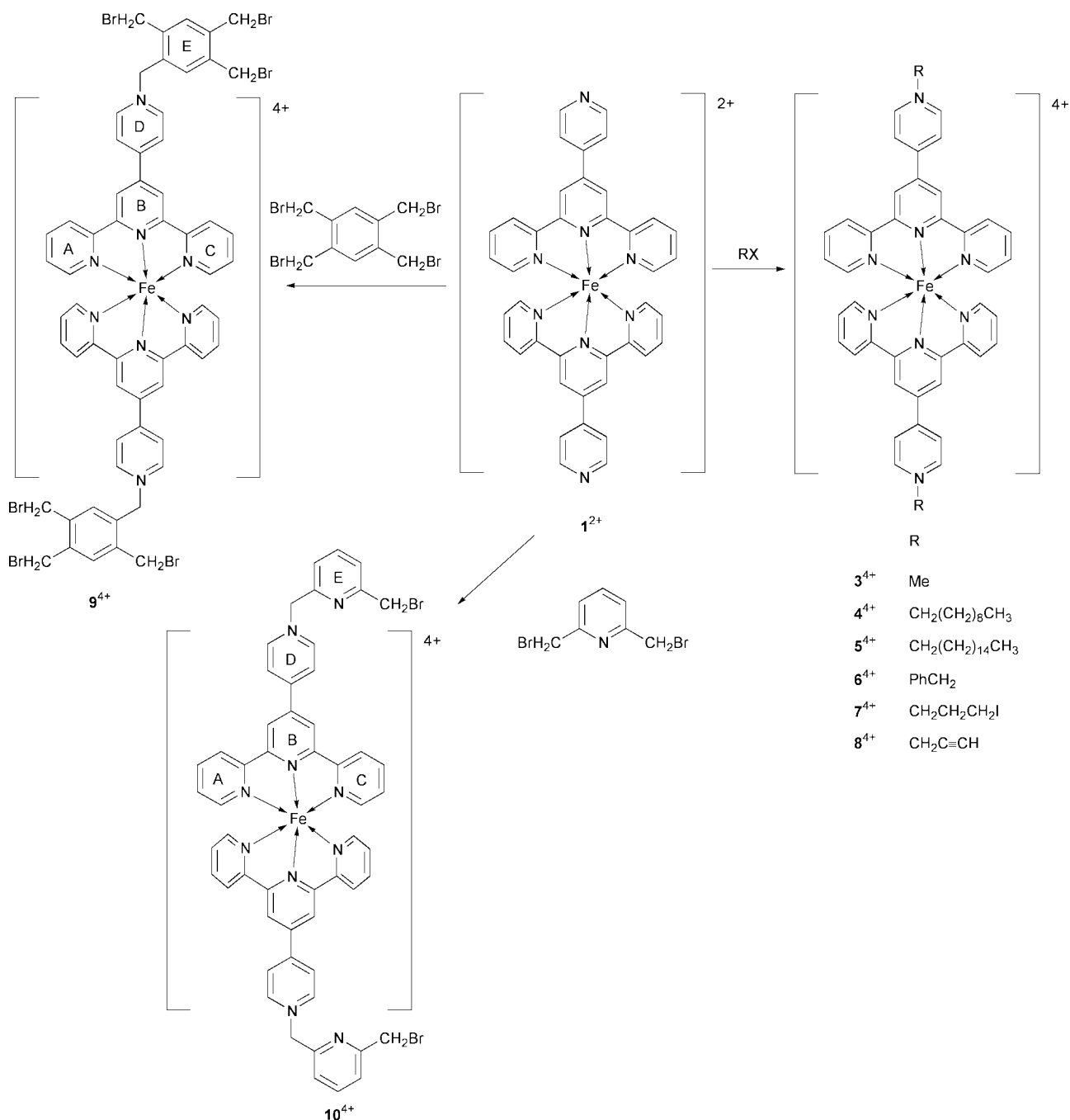


Fig. 4 Partial packing diagrams for VI[PF₆] showing (a) the stacking interaction between phenyl rings of adjacent VI⁺ cations, (b) the stacking of bipy domains of adjacent VI⁺ cations and (c) the snug fit of the cations into cavities. Hydrogen atoms have been omitted for clarity.

the colour change from purple to blue is characteristic and allows the reaction progress to be monitored. Analogous reactions with a variety of other alkylating agents in MeCN or mixtures of MeCN and CH₂Cl₂ or MeOCH₂CH₂OMe established that this was a general reaction and the *N*-alkylated complexes were isolated as deep blue or purple solids in respectable yields (Scheme 2). The parent methylated compound 3[PF₆]₄ together with 4[PF₆]₄, 5[PF₆]₄ and 6[PF₆]₄ were prepared by alkylation with the appropriate monofunctional alkyl halide followed by precipitation of the hexafluorophosphate salts with [NH₄][PF₆]. Encouraged by the success of these reactions we then extended the method to reaction with multifunctional halo compounds. The reaction of 1[PF₆]₂ with propargyl bromide gave the bis(alkyne) functionalised compound 7[PF₆]₄ whilst pendant electrophilic sites were introduced into 8[PF₆]₄, 9[PF₆]₄ and 10[PF₆]₄ by reaction with 1,3-diiodopropane, 1,2,4,5-tetrakis(bromomethyl)benzene or 2,6-bis(bromomethyl)pyridine respectively.

Direct preparation of *N*-alkylated complexes from *N*-alkylated ligands

As established in the preceding sections, it had proved to be possible to regiospecifically alkylate 1 at the pendant 4-pyridyl ring to give the free *N*-alkylated ligands IV[PF₆], V[PF₆] and VI[PF₆]. Additional evidence for the site of alkylation of these ligands comes from the direct reaction of IV[PF₆] with iron(II) salts to give deep blue complexes containing 3⁴⁺ salts, identical



Scheme 2

in all respects with those obtained from the methylation of $1[\text{PF}_6]_2$ ¹¹ (Scheme 1).

Characterisation of *N*-alkylated complexes $3[\text{PF}_6]_4$ – $10[\text{PF}_6]_4$

The properties of the *N*-alkylated complexes proved to be similar. The blue colour arises from a red-shifting of the MLCT absorption by some 25 nm to lower energy with respect to purple-red $1[\text{PF}_6]_2$ (λ_{max} 569 nm) and all of the alkylated complexes have λ_{max} (MLCT) in the range 595–597 nm. The shift in λ_{max} is due to a lowering of the energy of the LUMO (a ligand π^* -level) upon alkylation.

As expected, the complexes are redox active (Table 1) and show reversible or near reversible iron(II)/III processes in the range +0.82 to +0.89 V versus Fc/Fc^+ . These compare favourably with the potential of +0.89 V observed in $3[\text{PF}_6]_2$ and correspond to a destabilisation of the iron(III) state with respect to $1[\text{PF}_6]_2$ (+0.80 V) upon *N*-alkylation. In addition, each complex showed a number of quasi-reversible ligand reductions

with the exception of $5[\text{PF}_6]_4$ which exhibited strong absorption and desorption processes. The absorption process with $5[\text{PF}_6]_4$ was accompanied by the formation of a blue film on the electrode surface. The difference between the first metal-centred process and the first ligand-centred process is related to the HOMO–LUMO gap and correlates well with the observed MLCT absorptions ($[\text{Fe}(\text{terpy})_2]^{2+}$, $E_{\text{M}} - E_{\text{L}} = 2.38$ V, $\lambda_{\text{max}} = 551$ nm (≈ 2.25 V); $[\text{Fe}(\mathbf{1})_2]^{2+}$, $E_{\text{M}} - E_{\text{L}} = 2.31$ V, $\lambda_{\text{max}} = 569$ nm (≈ 2.18 V); $[\text{Fe}(\text{L})_2]^{4+}$, $E_{\text{M}} - E_{\text{L}} = 1.86$ – 1.93 V, $\lambda_{\text{max}} = 595$ – 597 nm (≈ 2.05 – 2.10 V)). The second ligand reduction potential was found to be dependent upon the working electrode (glassy carbon or platinum) in some cases.

The ^1H NMR spectra of CD_3CN solutions of the complexes are sharp and well-resolved and confirm that the compounds are symmetrical on the NMR time-scale. The NMR data suggest a considerable degree of charge localization since the chemical shifts of the protons on the terminal rings of the terpy in $\mathbf{1}^{2+}$ and the $[\text{Fe}(\text{L})_2]^{4+}$ compounds are almost constant. In contrast, significant downfield shifts of $\text{H}^{3\text{A}}$ (≈ 0.1 ppm), $\text{H}^{2\text{D}}$

(0.05–0.17 ppm) and H^{3D} (≈ 0.65 ppm) are observed upon *N*-alkylation of 1^{2+} . As expected, the chemical shifts of H^{2D} and H^{3D} are dependent upon the precise nature of the alkyl substituent. The additional protons within the substituents were observed at the expected chemical shifts. The 1H NMR spectrum of a CD_3CN solution of $6[PF_6]_4$, which is the model for the desired metallocycle, is presented in Fig. 5.

Structural characterisation of $1[NO_3]_2$ and $6[PF_6]_4$

Although attempts to grow good quality crystals of the salt $1[PF_6]_2$ only gave very small poor quality solids, in the course of investigating the coordination chemistry of the pendant 4-pyridyl group, we obtained reasonable quality crystals of $1[NO_3]_2 \cdot 3H_2O \cdot MeCN$ from the reaction of $1[PF_6]_2$ with cadmium nitrate. The X-ray structure of the 1^{2+} cation in this salt is presented in Fig. 6. The structural determination confirms that the gross structural features of the cation are as expected, with all bond lengths and angles within the coordination sphere and within the ligand being within normal limits (Table 2). The terpy metal-binding domains are essentially planar with a maximum variation of the least squares planes being 1.7° . Three features are, however, of interest. Firstly, the structural analysis allows a quantification of the analogy between the 1^{2+} cation and 4,4'-bipyridine. The linear arrangement of the two pendant 4-pyridyl groups is confirmed and the $N \cdots N$ distance is found to be 17.847 Å, considerably longer than those of 7.097 and 7.120 Å in 4,4'-bipyridine itself.¹⁹ Secondly, although the two pendant pyridyl groups are essentially linear ($\angle N(8)–Fe(1)–N(4) = 177.98^\circ$) the two rings are not exactly coplanar and are twisted with least squares planes of 8.56° with respect to each

other and form interplanar angles of about 40.64° and 39.73° with the B ring of the terpy ligand (Fig. 7a). These may be compared with least squares plane angles of 34.87 and 18.50° in 4,4'-bipyridine.¹⁹ The analogy between the 1^{2+} cation and 4,4'-bipyridine is good, with the metal complex representing an expanded form of the compound. Finally, there are π -stacking interactions between exactly coplanar terminal terpy rings of adjacent cations which form pairs with interplanar distances of 3.390 Å and centroid to centroid distances of 4.041 Å (Fig. 7b).

Good quality crystals of the complex $6[PF_6]_4 \cdot 2MeCN$ were also obtained and the structure of the 6^{4+} cation is presented in Fig. 8. Once again, all bond lengths and angles within the cation are within the usual limits (Table 2), although the terpy metal-binding domain is not so regular as in the 1^{2+} cation. Of the two terpy domains in the cation, one has A–B least squares plane angles of 3.45 and 3.94° whereas the other is more distorted with angles of 7.16 and 10.51° . The least squares plane angles of the B–D rings of 40.88 and 35.60° closely resemble those in 1^{2+} , and the approximate linearity of the core motif is maintained with $\angle N(8)–Fe(1)–N(7) = 165.90^\circ$, the

Table 2 Selected bond lengths (Å) and angles ($^\circ$) for $1[NO_3]_2 \cdot 3H_2O \cdot MeCN$ and $6[PF_6]_4 \cdot 2MeCN$

$1[NO_3]_2 \cdot 3H_2O \cdot MeCN$		$6[PF_6]_4 \cdot 2MeCN$	
Fe(1)–N(1)	1.976(4)	Fe(1)–N(5)	1.877(7)
Fe(1)–N(2)	1.879(4)	Fe(1)–N(2)	1.883(7)
Fe(1)–N(3)	1.978(4)	Fe(1)–N(6)	1.965(8)
Fe(1)–N(5)	1.974(4)	Fe(1)–N(1)	1.980(7)
Fe(1)–N(6)	1.886(4)	Fe(1)–N(4)	1.983(7)
Fe(1)–N(7)	1.969(5)	Fe(1)–N(3)	1.983(7)
C(5)–C(6)	1.468(6)	C(5)–C(6)	1.473(12)
C(8)–C(16)	1.479(8)	C(8)–C(25)	1.470(11)
C(10)–C(11)	1.462(7)	C(10)–C(11)	1.469(11)
C(25)–C(26)	1.466(7)	C(16)–C(22)	1.437(12)
C(28)–C(36)	1.484(8)	C(32)–C(33)	1.453(12)
C(30)–C(31)	1.467(7)	C(35)–C(52)	1.500(12)
		C(37)–C(38)	1.481(13)
		C(48)–C(49)	1.504(13)
N(1)–Fe(1)–N(2)	80.77(18)	N(5)–Fe(1)–N(2)	175.5(3)
N(1)–Fe(1)–N(3)	161.71(18)	N(5)–Fe(1)–N(6)	80.7(3)
N(1)–Fe(1)–N(5)	91.96(18)	N(2)–Fe(1)–N(6)	103.4(3)
N(1)–Fe(1)–N(6)	99.16(18)	N(5)–Fe(1)–N(1)	101.4(3)
N(1)–Fe(1)–N(7)	91.55(19)	N(2)–Fe(1)–N(1)	80.4(3)
N(2)–Fe(1)–N(3)	80.94(18)	N(6)–Fe(1)–N(1)	92.2(3)
N(2)–Fe(1)–N(5)	99.46(19)	N(5)–Fe(1)–N(4)	81.2(3)
N(2)–Fe(1)–N(6)	179.56(18)	N(2)–Fe(1)–N(4)	94.7(3)
N(2)–Fe(1)–N(7)	98.7(2)	N(6)–Fe(1)–N(4)	161.8(3)
N(3)–Fe(1)–N(5)	90.56(18)	N(1)–Fe(1)–N(4)	90.7(3)
N(3)–Fe(1)–N(6)	99.14(18)	N(5)–Fe(1)–N(3)	97.7(3)
N(3)–Fe(1)–N(7)	91.68(19)	N(2)–Fe(1)–N(3)	80.7(3)
N(5)–Fe(1)–N(6)	80.98(19)	N(6)–Fe(1)–N(3)	89.0(3)
N(5)–Fe(1)–N(7)	161.84(19)	N(1)–Fe(1)–N(3)	160.8(3)
N(6)–Fe(1)–N(7)	80.9(2)	N(4)–Fe(1)–N(3)	94.1(3)
		C(16)–C(22)–N(7)	115.8(9)
		N(8)–C(49)–C(48)	110.6(7)

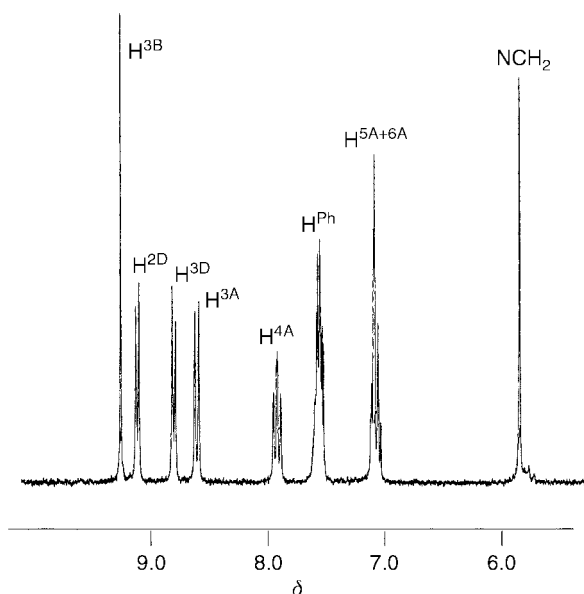


Fig. 5 250 MHz 1H NMR spectrum of a CD_3CN solution of $6[PF_6]_4$.

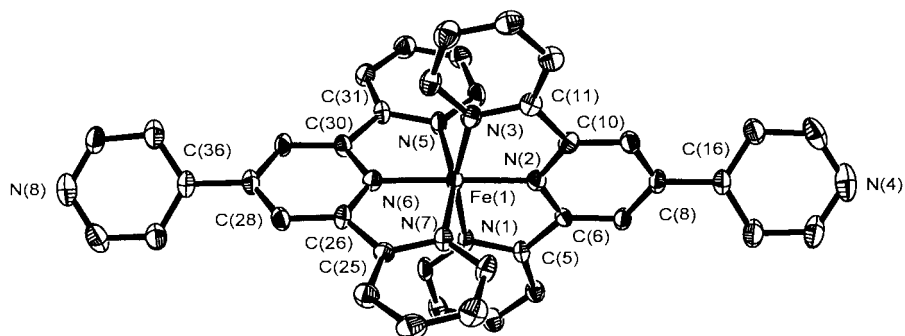


Fig. 6 Molecular structure of the 1^{2+} cation in the salt $1[NO_3]_2 \cdot 3H_2O \cdot MeCN$ showing the numbering scheme adopted. For clarity, only carbon atoms at the ring bridging sites are explicitly labelled (the numbering runs sequentially around each ring) and hydrogen atoms have been omitted; thermal ellipsoids at 50% probability.

deviation occurring as a result of the distortions within the less planar terpy motif.

Our interest in this compound is centred upon it as a model for the planned metallocycles and the orientation of the benzyl groups is of particular importance. The N(7)⋯N(8) distance within each cation is 17.536 Å; the slight decrease with respect to 1^{2+} is due to the deviations from planarity within 6^{4+} . The two benzyl groups are non-equivalent and the D ring–CH₂–Ph angles are 110.6(7) and 115.8(9)°. The phenyl rings are orientated in the same general direction, as required for the formation of 2^{8+} ; however, they are not orthogonal but are skewed outwards (C(48)–C(49)⋯C(22)–C(16) = 31.2°, least squares planes E–E', 61.48°).

These structural studies confirm that the proposed similarity between viologens and metalloviologens is good and the spatial

arrangement of the benzyl substituents in $6[\text{PF}_6]_4 \cdot 2\text{MeCN}$ is appropriate for the formation of the desired box 2^{8+} .

Reactivity of electrophilic metalloviologens

In a final step, we have investigated the reactivity of the pendant electrophilic functionality in 10^{4+} . A number of strategies may be envisaged for the preparation of the box compounds, and in some of the possible routes, an electrophilic complex will be closed by reaction with 1^{2+} . In this paper we describe one example of such a reaction, in which 10^{4+} is reacted with the nucleophile 4-ethylpyridine.

The reaction of $10[\text{PF}_6]_4$ with 4-ethylpyridine in MeCN gave a deep blue solution from which the complex $11[\text{PF}_6]_6$ was isolated in good yield (Scheme 3). This complex was fully characterised and exhibited the expected spectroscopic properties. The ¹H NMR spectrum of a solution of $11[\text{PF}_6]_6$ was well-resolved (Fig. 9) and showed a significant down-field shift of the H^{3B} protons with respect to $10[\text{PF}_6]_4$. This indicates that there is a significant structural/electronic change upon reaction of the remote site. However, the important observation, is that the reactivity of the pendant sites is not dramatically modified

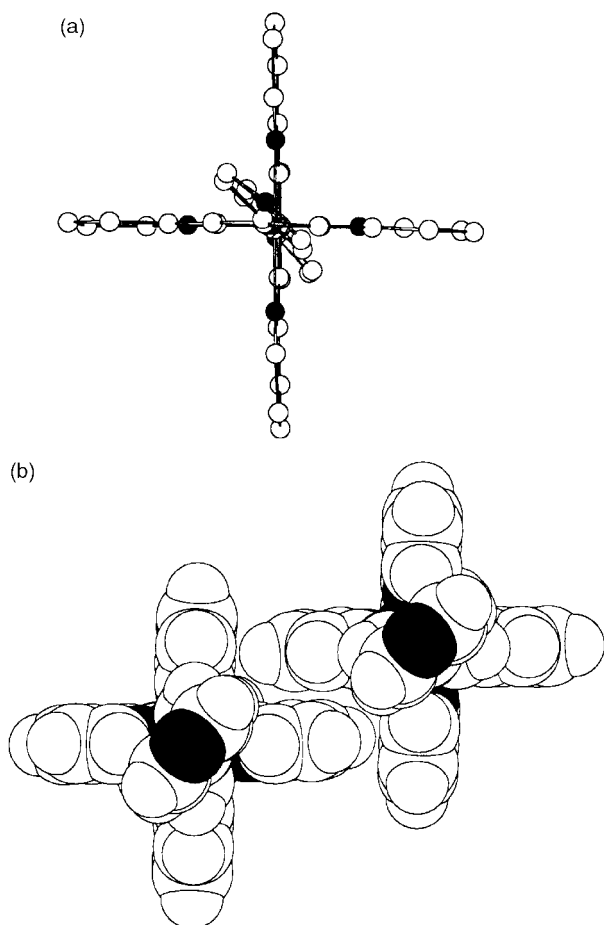


Fig. 7 (a) Molecular structure of the 1^{2+} cation in the salt $1[\text{NO}_3]_2 \cdot 3\text{H}_2\text{O} \cdot \text{MeCN}$ showing the relative orientation of the pendant D ring and the terpy metal-binding domains and (b) a space-filling representation showing the packing of the cations.

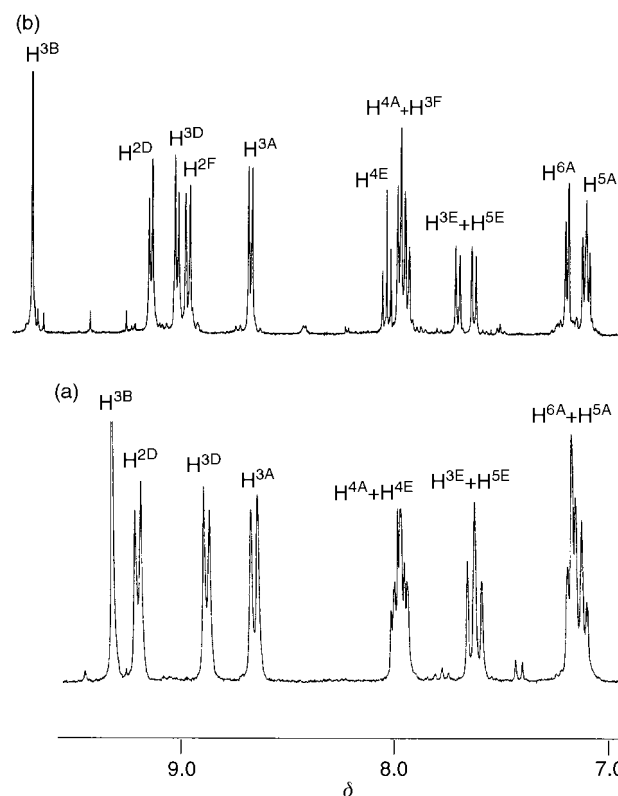


Fig. 9 ¹H NMR spectra of CD₃CN solutions of (a) $10[\text{PF}_6]_4$ (250 MHz) and (b) $11[\text{PF}_6]_6$ (400 MHz).

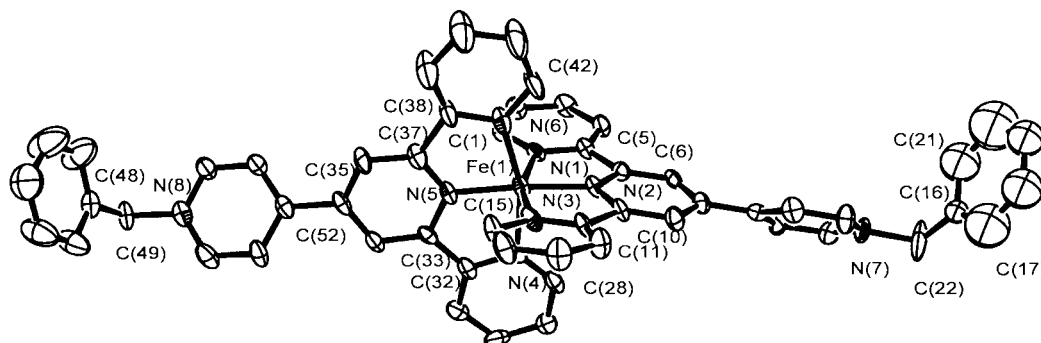
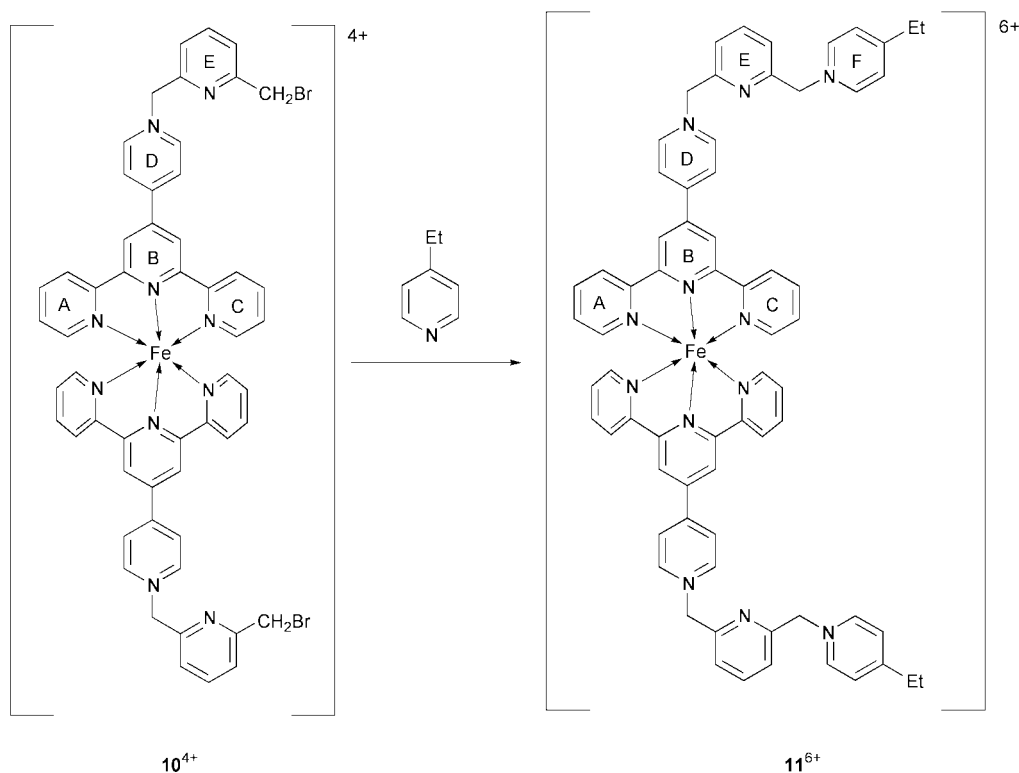


Fig. 8 Molecular structure of the 6^{4+} cation in the salt $6[\text{PF}_6]_4 \cdot 2\text{MeCN}$ showing the numbering scheme adopted. For clarity, only carbon atoms at the ring bridging sites (the numbering runs sequentially around each ring) and within the benzyl groups are explicitly labelled; hydrogen atoms have been omitted; thermal ellipsoids at 50% probability.



Scheme 3

upon incorporation into the complex.²⁰ Interestingly, although the ¹H NMR spectrum indicates a degree of interaction, the iron(II)/(III) redox potentials of **10**[PF₆]₄ and **11**[PF₆]₆ proved to be identical.

Conclusions

The analogy between the complex **1**²⁺ and 4,4'-bipyridine appears to be good; the complex undergoes *N*-alkylation reactions at the non-coordinated nitrogen atoms to generate metalloviologens. Structural studies reveal that the *N*-benzylated compounds possess the correct spatial characteristics for the formation of metallocycles related to cyclic bis(4,4'-bipyridinium) salts.

Experimental

Infrared spectra were recorded on Mattson Genesis Fourier-transform spectrophotometers with samples in compressed KBr discs. ¹H NMR spectra were recorded on Bruker AM 250 or 400 MHz spectrometers. UV/VIS measurements were performed using a Perkin-Elmer Lambda 19 spectrophotometer and were recorded in acetonitrile at a concentration of 5×10^{-5} M. FAB and EI mass spectra were recorded on a Kratos MS50 instrument. Time of flight (MALDI) spectra were recorded using a PerSeptive Biosystems Voyager-RP Biospectrometry Workstation. Electrochemical measurements were performed with an Amel model 553 potentiostat connected to an Amel model 567 function generator and an Amel model 560/A interface or an Eco Chemie Autolab PGSTAT 20 system using platinum bead working and auxiliary electrodes with an Ag/AgCl electrode as reference. The experiments were conducted using purified acetonitrile as solvent and 0.1 M [Buⁿ₄N][BF₄] as supporting electrolyte; ferrocene was added at the end of each experiment as an internal reference.

Preparations

4'-(*N*-Methyl-4-pyridinio)-2,2':6',2''-terpyridine hexafluorophosphate IV[PF₆]. MeI (0.3 cm³, 4.8 mmol) was added to a

solution of **I** (0.180 g, 0.6 mmol) in MeCN (50 cm³) and the mixture heated to reflux for 12 h to give a yellow solution which was concentrated to ≈ 10 cm³ volume and treated with aqueous [NH₄][PF₆] to give **IV**[PF₆] as a yellow powder (0.120 g, 44%), mp >250 °C (Found: C, 52.1; H, 3.9; N, 11.67. C₂₁H₁₇F₆N₄P·0.5H₂O requires C, 52.6; H, 3.8; N, 11.79%); δ_{H} (CDCl₃) 8.88 (2H, m, H^{3B}), 8.71–8.78 (6H, m, H^{6A,2D,3A}), 8.45 (2H, d, H^{3D}), 8.01 (2H, td, H^{4A}), 7.50 (2H, ddd, H^{5A}), 4.36 (3H, s, CH₃); δ_{C} (CD₃CN) 155.5, 150.3, 146.7, 138.5, 126.9, 125.8, 122.2, 119.8, 118.1, 117.6, 117.5, 44.0; $\tilde{\nu}_{\text{max}}$ /cm⁻¹ 3117w, 3050w, 1646m, 1583m, 1549m, 1525m, 1392s, 1338w, 1190m, 1089m, 833s, 791s, 745w, 657w, 558s (KBr); m/z 325 (M⁺), 310 (M – Me) (FAB); λ_{max} /nm (MeCN) 254 (ϵ/M^{-1} cm⁻¹ 33.18×10^3), 276 (32.58×10^3), 337 (4.93×10^3).

4'-(*N*-Ethyl-4-pyridinio)-2,2':6',2''-terpyridine hexafluorophosphate V[PF₆]. A solution of **I** (0.192 g, 0.62 mmol) was heated in freshly distilled CH₃CN (50 cm³) and bromoethane (50 cm³) for 48 h after which [NH₄][PF₆] was added to the cooled reaction mixture, the solvent removed *in vacuo* and the product recrystallised from acetone/EtOH to give **V**[PF₆] as a yellow solid (0.071 g, 24%), mp >250 °C (Found: C, 54.4; H, 4.5; N, 12.8. C₂₂H₁₉F₆N₄P·CH₃CN·CH₃OH requires C, 53.9; H, 4.7; N, 12.69%); δ_{H} (CD₃CN) 8.84 (2H, s, H^{3B}), 8.82 (2H, d, H^{2D}), 8.74 (2H, d, H^{6A}), 8.71 (2H, d, H^{3A}), 8.46 (2H, d, H^{3D}), 8.01 (2H, ddd, H^{4A}), 7.50 (2H, ddd, H^{5A}), 4.64 (2H, q, H^{CH₂}), 1.65 (3H, t, H^{CH₃}); δ_{C} (CD₃CN) 157.9, 155.6, 155.4, 150.4, 145.7, 144.8, 138.6, 127.3, 125.9, 122.3, 119.8, 58.0 (CH₂), 16.7 (CH₃); m/z 340 (M – PF₆) (MALDI-TOF); $\tilde{\nu}_{\text{max}}$ /cm⁻¹ 3133w, 3068w, 3002, 1644m, 1584m, 1567m, 1549m, 1522m, 1471m, 1454w, 1393m, 1345w, 1267w, 1177, 1089w, 850s, 792m, 752w, 682w, 558 (KBr); λ_{max} /nm (MeCN) 275 (ϵ/M^{-1} cm⁻¹ 38.2×10^3), 334 (5.0×10^3).

4'-(*N*-Benzyl-4-pyridinio)-2,2':6',2''-terpyridine hexafluorophosphate VI[PF₆]. **I** (0.109 g, 0.35 mmol) was heated in freshly distilled CH₃CN (100 cm³) with PhCH₂Br (0.300 g, 1.75 mmol) for 4 h; following addition of [NH₄][PF₆] to the cooled reaction mixture, the product was collected by filtration, washed with hexane and water and purified by vapour diffusion of diiso-

propyl ether into an MeCN solution to give yellow plates of **VI**[PF₆]₄ (0.167 mg, 87%), mp >250 °C (Found: C, 58.7; H, 4.3; N, 11.0. C₂₇H₂₁F₆N₄P·CH₃CN·CH₃OH requires C, 58.2; H, 4.5; N, 11.3%); δ_H (CD₃CN) 8.84 (2H, s, H^{3B}), 8.87 (2H, d, H^{2D}), 8.73 (2H, d, H^{6A}), 8.70 (2H, d, H^{3A}), 8.46 (2H, d, H^{3D}), 8.00 (2H, ddd, H^{4A}), 7.51 (5H, s, H^{Ph}), 7.49 (2H, ddd, H^{5A}), 5.78 (2H, s, H^{CH}); δ_C (CD₃CN) 157.9, 155.9, 155.5, 150.2, 145.7, 144.5, 138.2, 133.7, 130.8, 130.4, 129.9, 127.3, 125.6, 122.0, 119.6, 65.0 (CH₂); *m/z* 402 (M - PF₆) (MALDI-TOF); ν_{max}/cm⁻¹ 3134w, 3062w, 1639m, 1603w, 1584m, 1567m, 1550m, 1520m, 1470m, 1393m, 1160m, 840s, 791s, 745m, 701m, 686w, 558s (KBr); λ_{max}/nm (MeCN) 275 (ε/M⁻¹ cm⁻¹ 63.2 × 10³), 338 (7.9 × 10³).

3[PF₆]₄. Solid [Fe(H₂O)₆][BF₄]₂ (15.1 mg, 0.06 mmol) was added to a solution of **IV**[PF₆]₄ (56.4 mg, 0.12 mmol) in MeCN (10 cm³) and the mixture stirred at room temperature for 1 h to give a deep blue solution which was then treated with aqueous [NH₄][PF₆] to give a deep blue precipitate. This was collected by filtration and dried under high vacuum to give **2**[PF₆]₄ in quantitative yield. δ_H (CD₃CN) 9.31 (4H, s, H^{3B}), 9.02 (4H, d, H^{2D}), 8.84 (4H, d, H^{3D}), 8.67 (4H, d, H^{3A}), 7.98 (4H, ddd, H^{4A}), 7.21 (4H, d, H^{6A}), 7.14 (4H, ddd, H^{5A}), 4.52 (6H, s, CH₃); *m/z* 705 (M - 2PF₆) (FAB); λ_{max}/nm (MeCN) 255 (ε/M⁻¹ cm⁻¹ 39.3 × 10³), 282 (55.1 × 10³), 290 (56.7 × 10³), 334 (20.4 × 10³), 378sh (6.9 × 10³), 599 (18.4 × 10³).

N-Alkylation of 1[PF₆]₂. *Method 1* (C₁₀H₂₁Br, C₁₆H₃₃Br, HC≡CCH₂Br and I(CH₂)₃I). A solution of **1**[PF₆]₂ (40 mg, 0.041 mmol) and the alkyl halide (1 cm³) in MeCN or 1:1 MeCN:MeOCH₂CH₂OMe (30 cm³) was heated to reflux for 24–40 h to give blue solutions which were concentrated to ≈10 cm³ volume and treated with methanolic [NH₄][PF₆] to give the products **4**[PF₆]₄, **5**[PF₆]₄, **7**[PF₆]₄ and **8**[PF₆]₄ as deep blue microcrystalline solids (70–90%).

Method 2 (PhCH₂Br, 1,2,4,5-(BrCH₂)₄C₆H₂) and 2,6-(BrCH₂)₂py. A solution of **1**[PF₆]₂ (30 mg, 0.031 mmol) and the alkyl halide (1.1 mmol) in 2:1 MeCN:CH₂Cl₂ (30 cm³) was stirred at room temperature for 4 h to give deep blue solutions which were worked up as above to give **6**[PF₆]₄, **9**[PF₆]₄ or **10**[PF₆]₄ as deep blue microcrystalline solids (60–80%).

4[PF₆]₄. (Found: C, 45.1; H, 4.9; N, 6.9. C₆₀H₇₀F₂₄FeN₈P₄·3H₂O requires C, 45.2; H, 4.8; N, 7.0%); δ_H (CD₃CN) 9.29 (s, 4H, H^{3B}), 9.06 (d, 4H, H^{2D}), 8.85 (d, 4H, H^{3D}), 8.66 (d, 4H, H^{3A}), 7.97 (dt, 4H, H^{4A}), 7.20 (dd, 4H, H^{6A}), 7.14 (dd, 4H, H^{5A}), 4.72 (t, 4H, NCH₂), 1.2–1.6 (m, 38H, (CH₂)₈CH₃); *m/z* 1394 (M - PF₆), 1249 (M - 2PF₆), 1104 (M - 3PF₆) (FAB); ν_{max}/cm⁻¹ 1642s, 1577m, 1540m, 1457m, 1425m, 1363m, 1289m, 1180w, 1027m, 835s, 789m, 751m, 557s, 459m (KBr); λ_{max}/nm (MeCN) 276 (ε/M⁻¹ cm⁻¹ 297.7 × 10³), 284 (285.6 × 10³), 328 (50.3 × 10³), 345sh (37.7 × 10³), 379 (18.7 × 10³), 595 (41.2 × 10³).

5[PF₆]₄. (Found: C, 48.6; H, 5.4; N, 6.1. C₇₂H₉₄F₂₄FeN₈P₄·3H₂O requires C, 49.1; H, 5.7; N, 6.4%); δ_H (CD₃CN) 9.28 (s, 4H, H^{3B}), 9.06 (d, 4H, H^{2D}), 8.84 (d, 4H, H^{3D}), 8.66 (s, 4H, H^{3A}), 7.97 (dt, 4H, H^{4A}), 7.20 (dd, 4H, H^{6A}), 7.14 (dd, 4H, H^{5A}), 4.72 (t, 4H, NCH₂), 1.2–1.6 (m, 62H, (CH₂)₁₄CH₃); *m/z* 1562 (M - PF₆), 1417 (M - 2PF₆), 1272 (M - 3PF₆) (FAB); ν_{max}/cm⁻¹ 1641s, 1577m, 1543m, 1460m, 1425m, 1362w, 1290m, 1245m, 1179m, 1029m, 837s, 789m, 752w, 558s, 458m (KBr); λ_{max}/nm (MeCN) 275 (ε/M⁻¹ cm⁻¹ 204.8 × 10³), 284 (196.7 × 10³), 328 (41.8 × 10³), 345sh (32.6 × 10³), 379 (16.1 × 10³), 595 (38.3 × 10³).

7[PF₆]₄. (Found: C, 38.7; H, 2.7; N, 7.7. C₄₆H₃₄F₂₄FeN₈P₄·4H₂O requires C, 39.3; H, 3.0; N, 8.0%); δ_H (CD₃CN) 9.33 (s, 4H, H^{3B}), 9.23 (d, 4H, H^{2D}), 8.90 (d, 4H, H^{3D}), 8.67 (s, 4H, H^{3A}), 7.97 (dt, 4H, H^{4A}), 7.18 (dd, 4H, H^{6A}), 7.15 (dd, 4H, H^{5A}), 5.63 (s, 4H, NCH₂), 3.42 (s, 2H, ≡CH); *m/z* 1189 (M - PF₆), 1045

(M - 2PF₆), 899 (M - 3PF₆) (FAB); ν_{max}/cm⁻¹ 3305m, 2132w, 1638s, 1610m, 1534m, 1522m, 1426s, 1364m, 1291m, 1246m, 1163m, 1029m, 836s, 789m, 755m, 557s (KBr); λ_{max}/nm (MeCN) 276 (ε/M⁻¹ cm⁻¹ 229.7 × 10³), 284 (215.9 × 10³), 329 (48.1 × 10³), 346sh (32.3 × 10³), 381 (17.5 × 10³), 596 (40.4 × 10³).

8[PF₆]₄. (Found: C, 32.2; H, 2.6; N, 6.4. C₄₆H₄₂F₂₄FeN₈P₄·HI·CH₃OH requires C, 32.2; H, 2.6; N, 6.4%); δ_H (CD₃CN) 9.29 (s, 4H, H^{3B}), 9.08 (d, 4H, H^{2D}), 8.86 (d, 4H, H^{3D}), 8.66 (s, 4H, H^{3A}), 7.97 (dt, 4H, H^{4A}), 7.19 (dd, 4H, H^{6A}), 7.14 (dd, 4H, H^{5A}), 4.81 (t, 4H, NCH₂), 3.38 (m, 4H, CH₂I), 2.68 (t, 4H, CH₂CH₂); *m/z* 1449 (M - PF₆), 1306 (M - 2PF₆), 1159 (M - 3PF₆) (FAB); ν_{max}/cm⁻¹ 1640s, 1577m, 1542m, 1458w, 1425m, 1363m, 1289m, 1244m, 1180m, 1029m, 835s, 789m, 752m, 557s, 458m (KBr); λ_{max}/nm (MeCN) 275 (ε/M⁻¹ cm⁻¹ 234.3 × 10³), 283 (224.8 × 10³), 329 (43.9 × 10³), 345sh (33.4 × 10³), 380 (16.3 × 10³), 596 (39.9 × 10³).

6[PF₆]₄. (Found: C, 42.9; H, 3.1; N, 7.2. C₅₄H₄₂F₂₄FeN₈P₄·3H₂O requires C, 42.9; H, 3.3; N, 7.4%); δ_H (CD₃CN) 9.27 (s, 4H, H^{3B}), 9.13 (d, 4H, H^{2D}), 8.82 (d, 4H, H^{3D}), 8.63 (s, 4H, H^{3A}), 7.96 (dt, 4H, H^{4A}), 7.60 (m, 10H, H^{Ph}), 7.18 (dd, 4H, H^{6A}), 7.13 (dd, 4H, H^{5A}), 5.92 (s, 4H, NCH₂); *m/z* 1294 (M - PF₆), 1149 (M - 2PF₆), 1004 (M - 3PF₆) (FAB); ν_{max}/cm⁻¹ 1640s, 1576m, 1542m, 1461w, 1425m, 1364w, 1289m, 1245m, 1180m, 1032m, 837s, 789m, 752w, 558s, 459w (KBr); λ_{max}/nm (MeCN) 275 (ε/M⁻¹ cm⁻¹ 140.1 × 10³), 283 (134.6 × 10³), 329 (22.5 × 10³), 345sh (16.8 × 10³), 382 (8.2 × 10³), 597 (21.5 × 10³).

9[PF₆]₄. (Found: C, 33.2; H, 2.95; N, 5.0. C₆₀H₄₈Br₆F₂₄FeN₈P₄·10H₂O requires C, 33.1; H, 3.15; N, 5.15%); δ_H (CD₃CN) 9.61 (s, 4H, H^{3B}), 9.20 (d, 4H, H^{2D}), 9.18 (d, 4H, H^{3D}), 8.90 (s, 4H, H^{3A}), 7.95 (dt, 4H, H^{4A}), 7.73 (s, 2H, H^{6E}), 7.57 (s, 2H, H^{3E}), 7.19 (dd, 4H, H^{6A}), 7.12 (dd, 4H, H^{5A}), 6.12 (s, 4H, NCH₂), 4.83 (s, 4H, 2-CH₂Br), 4.78 (s, 8H, 4-CH₂Br, 5-CH₂Br); *m/z* 1851 (M - PF₆), 1706 (M - 2PF₆), 1561 (M - 3PF₆) (FAB); ν_{max}/cm⁻¹ 1638s, 1575m, 1539m, 1425m, 1368w, 1289m, 1243m, 1178m, 1028m, 839s, 790m, 558s, 461w (KBr); λ_{max}/nm (MeCN) 275 (ε/M⁻¹ cm⁻¹ 107.3 × 10³), 283 (96.2 × 10³), 328 (24.7 × 10³), 347sh (18.1 × 10³), 382 (9.1 × 10³), 597 (16.9 × 10³).

10[PF₆]₄. (Found: C, 37.3; H, 3.0; N, 7.8. C₅₄H₄₂Br₂F₂₄FeN₈P₄·6H₂O requires C, 37.4; H, 3.1; N, 8.1%); δ_H (CD₃CN) 9.32 (s, 4H, H^{3B}), 9.20 (d, 4H, H^{2D}), 8.88 (d, 4H, H^{3D}), 8.65 (s, 4H, H^{3A}), 7.98 (dt, 4H, H^{4A}), 7.97 (t, 2H, H^{4E}), 7.64 (d, 2H, H^{3E}), 7.61 (dd, 2H, H^{5E}), 7.18 (dd, 4H, H^{6A}), 7.13 (dd, 4H, H^{5A}), 6.03 (s, 4H, NCH₂), 4.57 (s, 4H, CH₂Br); *m/z* 1482 (M - PF₆), 1338 (M - 2PF₆), 1193 (M - 3PF₆) (FAB); ν_{max}/cm⁻¹ 1639s, 1577m, 1543m, 1458m, 1425m, 1365w, 1291m, 1246m, 1178m, 1029m, 836s, 789m, 752w, 558s, 458m (KBr); λ_{max}/nm (MeCN) 276 (ε/M⁻¹ cm⁻¹ 90 × 10³), 284 (86.4 × 10³), 329 (20.5 × 10³), 347sh (17.4 × 10³), 382 (8.2 × 10³), 597 (18.8 × 10³).

11[PF₆]₆. A solution of **10**[PF₆]₄ (40 mg, 0.024 mmol) in MeCN (20 cm³) was treated with 4-ethylpyridine (1.1 mmol) and the mixture refluxed for 20 h to give a deep blue solution which was then concentrated to ≈10 cm³ volume, methanolic [NH₄][PF₆] added, cooled and treated with diethyl ether to give a deep blue precipitate. This was collected by filtration and dried under high vacuum to give **11**[PF₆]₆ (38 mg, 75%) (Found: C, 38.0; H, 3.5; N, 7.5. C₆₈H₆₀F₃₆FeN₁₂P₆·6H₂O·HBr requires C, 37.8; H, 3.4; N, 7.8%); *m/z* 1826 (M - PF₆), 1681 (M - 2PF₆), 1536 (M - 3PF₆), 1391 (M - 4PF₆), 1246 (M - 5PF₆) (FAB); ν_{max}/cm⁻¹ 1641s, 1576m, 1545m, 1457m, 1422m, 1412m, 1365w, 1287m, 1243m, 1169m, 1031m, 841s, 791m, 752w, 560s, 459m (KBr); δ_H (CD₃CN) 9.71 (4H, s, H^{3B}), 9.16 (4H, d, H^{2D}), 9.04 (4H, d, H^{3D}), 8.98 (4H, d, H^{2E}), 8.70 (4H, d, H^{3A}), 8.07 (2H, t, H^{4E}), 8.01 (4H, d, H^{3E}), 7.98 (4H, td, H^{4A}), 7.74 (2H, d, H^{3E}), 7.67 (2H, d, H^{5E}), 7.24 (4H, d, H^{6A}), 7.15 (4H, td, H^{5A}), 5.95

Table 3 Crystallographic data for **1**[NO₃]₂·3H₂O·MeCN and **6**[PF₆]₄·2MeCN

	1 [NO ₃] ₂ ·3H ₂ O·MeCN	6 [PF ₆] ₄ ·2MeCN
Formula	C ₄₂ H ₃₇ FeN ₁₁ O ₉	C ₅₈ H ₄₈ F ₂₄ FeN ₁₀ P ₄
<i>M</i>	895.68	1520.79
Crystal system	Triclinic	Triclinic
Space group	<i>P</i> $\bar{1}$	<i>P</i> $\bar{1}$
μ/mm^{-1}	0.44	0.46
Final <i>R</i>	0.0923, 0.0872	0.1546, 0.0827
(all data, observed)		
Final <i>R</i> _w	0.2235, 0.2186	0.2177, 0.1736
(all data, observed)		
<i>a</i> /Å	12.4568(15)	15.844(9)
<i>b</i> /Å	15.476(2)	16.940(7)
<i>c</i> /Å	10.9876(13)	13.393(3)
α /°	96.259(8)	97.31(3)
β /°	98.240(5)	106.67(3)
γ /°	101.269(9)	65.50(3)
<i>V</i> /Å ³	2035.3	3133.4
<i>T</i> /K	150	150
<i>Z</i>	2	2
No. reflections	10792	8598
No. independent reflections	6372	8165
No. observed reflections	5955	4717
	<i>I</i> > 2σ(<i>I</i>)	<i>I</i> > 2σ(<i>I</i>)

(4H, s, NCH₂ {D–E}), 5.79 (4H, s, NCH₂ {E–F}), 2.97 (4H, q, CH₂CH₃), 1.25 (6H, t, CH₃).

Crystal structure determinations

The structures were solved and refined by direct methods using standard techniques as indicated in Table 3 using the programmes CRYSTALS,²¹ SHELXS-86,²² SHELX-93²³ and SHELXS-97.²⁴ Diagrams and supplementary material were prepared using the above programmes together with ORTEP-3 for Windows²⁵ and PLATON.^{26,27} The structure solution and refinement was routine except in the case of **1**[NO₃]₂·3H₂O·MeCN where considerable disorder of the solvent molecules was observed. As the interest lay in the cation, a model was adopted in which one of the water molecules was represented by an oxygen atom over three sites with 1/3 occupancy. The hydrogen atoms of two of the lattice water molecules and the lattice MeCN were not located.

CCDC reference number 186/1943.

See <http://www.rsc.org/suppdata/dt/b0/b000940g/> for crystallographic files in .cif format.

Acknowledgements

We thank the Schweizerischer Nationalfonds zur Förderung der wissenschaftlichen Forschung, the University of Basel, EPSRC and Ciba-Geigy for financial support of this work.

References

- E. C. Constable, in *Comprehensive Supramolecular Chemistry*, eds. J. L. Atwood, J. E. D. Davies, D. D. MacNicol and F. Vögtle, Pergamon Press, Oxford, 1996, vol. 9, p. 213 and references therein.
- C. Piguet, G. Bernardinelli and G. Hopfgartner, *Chem. Rev.*, 1997, **97**, 2005.
- M. Fujita, in *Comprehensive Supramolecular Chemistry*, eds. J. L. Atwood, J. E. D. Davies, D. D. MacNicol and F. Vögtle, Pergamon Press, Oxford, 1996, vol. 9, p. 253 and references therein.
- J.-C. Chambron, in *Transition Metals in Supramolecular Chemistry*, ed. J.-P. Sauvage, Wiley, Chichester, 1999, p. 225.
- R. W. Saalfrank and B. Demleitner, in *Transition Metals in Supramolecular Chemistry*, ed. J.-P. Sauvage, Wiley, Chichester, 1999, p. 1.
- P. J. Stang and B. Olenyuk, *Acc. Chem. Res.*, 1997, **30**, 502; P. J. Stang, *Chem. Eur. J.*, 1998, **4**, 19.
- P. N. W. Baxter, in *Comprehensive Supramolecular Chemistry*, eds. J. L. Atwood, J. E. D. Davies, D. D. MacNicol and F. Vögtle, Pergamon Press, Oxford, 1996, vol. 9, p. 165 and references therein.
- G. R. Newkome, E. He and C. N. Moorefield, *Chem. Rev.*, 1999, **99**, 1689.
- E. C. Constable, *Chem. Ind.*, 1994, 56; E. C. Constable and D. Smith, *Chem. Brit.*, 1995, **31**, 33.
- S. J. Dunne and E. C. Constable, *Inorg. Chem. Commun.*, 1998, **1**, 167; E. C. Constable and P. Harverson, *Polyhedron*, 1999, **18**, 1891; E. C. Constable and T. A. Leese, *Inorg. Chim. Acta*, 1988, **146**, 55; E. C. Constable, A. M. W. Cargill Thompson, P. Harverson, L. Macko and M. Zehnder, *Chem. Eur. J.*, 1995, **1**, 360.
- E. C. Constable and A. M. W. Cargill Thompson, *J. Chem. Soc., Dalton Trans.*, 1992, 2947; *J. Chem. Soc., Dalton Trans.*, 1994, 1409.
- E. C. Constable, *Metals and Ligand Reactivity. An Introduction to the Organic Chemistry of Metal Complexes*, VCH, Weinheim, 1995.
- D. Philp and J. F. Stoddart, *Angew. Chem.*, 1996, **108**, 1242; *Angew. Chem., Int. Ed. Engl.*, 1996, **35**, 1155.
- F. Kröhnke, *Synthesis*, 1976, 1.
- P. M. S. Monk, *The Viologens: Physicochemical Properties, Synthesis and Applications of Salts of 4,4'-bipyridine*, Wiley, Chichester, 1998 and references therein.
- E. C. Constable and E. Schofield, *Chem. Commun.*, 1998, 403.
- E. C. Constable, *Adv. Inorg. Chem. Radiochem.*, 1987, **30**, 69.
- R. A. Mackay, J. R. Randolph and E. J. Poziomek, *J. Am. Chem. Soc.*, 1971, **93**, 5026.
- N. M. Boag, K. M. Coward, A. C. Jones, M. E. Pemble and J. R. Thompson, *Acta Crystallogr., Sect. C*, 1999, **55**, 672.
- P. D. Beer, N. C. Fletcher, A. Grieve, J. W. Wheeler, C. P. Moore and T. Wear, *J. Chem. Soc., Perkin Trans. 2*, 1996, 1545.
- D. J. Watkin, J. R. Carruthers and P. Betteridge, CRYSTALS, Chemical Crystallography Laboratory, Oxford, UK, 1985.
- G. M. Sheldrick, SHELXS-86, Program for Crystal Structure Solution, University of Göttingen, Germany, 1986.
- G. M. Sheldrick, SHELX-93, Program for Crystal Structure Refinement, University of Göttingen, Germany, 1993.
- G. M. Sheldrick, SHELXS-97, Program for Crystal Structure Solution, University of Göttingen, Germany, 1986.
- L. J. Farrugia, ORTEP-3 for Windows, University of Glasgow, 1999.
- A. L. Spek, *Acta Crystallogr., Sect. A*, 1990, **46**, C-34.
- L. J. Farrugia, PLATON for Windows, University of Glasgow, 1999.